A method for estimation of equivalent-volume ice thickness based on WMO egg code in absence of ridging parameters

Aleksandar-Saša Milaković; Peter Schütz; Henry Piehl; Sören Ehlers

Accepted for publication in
Cold Regions Science and Technology
DOI: https://doi.org/10.1016/j.coldregions.2018.08.017

A method for estimation of equivalent-volume ice thickness based on WMO egg code in absence of ridging parameters

ABSTRACT

When calculating equivalent-volume ice thickness along a vessel's projected route for the purpose of ice resistance estimation, information on both undeformed ice (level ice) and deformed ice (mainly ridges) is needed. Level ice information can be obtained from egg code-based ice charts in form of World Meteorological Organization (WMO) ice thickness ranges. Ridging parameters are sometimes available in ice charts as a supplement to the egg code, but are often missing, especially for the areas in the Arctic, in which case area- and season-specific values of these parameters are obtained from the databases. In this paper, limitation of the latter approach is presented, showing that when the currently available ridging parameters for the Arctic are used, the expected amount of ice along the route underestimates the one measured by a submarine by 29%. As an alternative approach, a novel method for estimating the equivalent-volume ice thickness without requiring ridging parameters is presented. It proposes substitution of WMO ice thickness ranges (currently accounting only for the level ice) with equivalent-volume ice thickness ranges (EVITRs), accounting both for the level ice and for the deformed ice features. The method is based on correlating the amount of deformed ice to the stage of development of the ambient level ice, by analyzing a series of ice thickness profiles for a certain area and season. Consequently, the method provides a mean for the estimation of the total amount of ice and its components along the route based only on the information available in the egg code. The results of a case study in the Arctic show an increased accuracy of the EVITR-based method compared to the ridging parameters-based method, reducing the average error in estimation of the total amount of ice along the vessel's route from 29% to 2%.

Keywords: Arctic shipping; Equivalent ice thickness; Egg code; Ice charts; Ice ridges; Level ice; Submarine upward looking sonar.

1. INTRODUCTION

When calculating ship resistance in a complex ice field consisting of level ice, deformed ice features (ridges), and open water, two different approaches can be taken. First is to use high-fidelity transit simulations (e.g. Kuuliala et al., 2017; Li et al., 2018) where ship speed is calculated by solving equation of motion at every time step, taking the actual ice profile into account. The advantage of this approach is that it yields results of high accuracy, while the drawbacks are complexity of the models requiring high level of expertise to build and to use them, as well as the computational expensiveness. Second approach pertains to low-fidelity transit simulations (e.g. Valkonen and Riska, 2014; Bergström, 2016) where the actual ice profile is simplified using the concept of equivalent ice thickness (H), which averages the resistance effects of different ice features into a single thickness value. Ice resistance is then calculated in this simplified ice profile of constant thickness. The advantage of this approach lies in its simplicity since the complex ice conditions in an area can be described using only one parameter, making it applicable for engineering studies in early phases of ship design when the level of uncertainty is high, as well as for some specific types of calculations such as ship routing in ice.

The value of H in context of ship resistance calculations can be defined in two ways. First is the equivalent-volume ice thickness (H_v), which preserves the total volume of ice from the original ice profile (Leppäranta, 1980; Riska 2010). The value of H_v is such that the cross sectional area of the equivalent ice profile equals the cross sectional area of the original ice profile. Second is the equivalent-performance ice thickness (H_p), where H_p is equal to the level ice thickness producing the same resistance for a given ship as the complex ice profile in question (Riska, 2009). Clearly, calculation of H_p requires ship parameters to be known, while H_v can theoretically be applied to any ship.

In order to calculate H_v, several parameters describing the ice cover are needed: ice concentration, level ice thickness, and ridging parameters such as ridge dimensions and frequency of their occurrence. The first two can be obtained from ice charts, which use the so-called egg code to describe the ice cover. Egg code is a system for classification of ice conditions established by World Meteorological Organization (WMO, 1970) and consists of information about ice concentration (c), stage of development of ice (SOD) and floe

size, usually for three predominant ice categories in an area, each described by a different SOD. Each SOD is characterized by a WMO ice thickness range (WMOITR) indicating upper and lower limits of level ice thickness. WMOITRs do not take deformed ice into account. Ridging parameters – needed to describe the deformed ice – are sometimes available as a supplement to the egg code in ice charts. This is especially the case in the Baltic, due to a highly developed network used for detection of ice conditions and also a relatively small area. However, for large areas in the Arctic, the ridging parameters are usually missing from the ice charts. This is due to difficulties in obtaining them through remote sensing techniques such as synthetic aperture radars (SAR, see Bertoia et al., 2004), which are mainly used for developing ice charts for high-latitude areas (Sandven et al., 2006). When they are unavailable from the ice charts, ridging parameters can be obtained from one of the databases containing their area- and season-specific values, which are usually derived from in-field measurements recorded over longer period of time. Romanov (1995) developed one of the most widely used databases of such values for the Arctic. The accuracy of calculations when ridging parameters are obtained from such databases can be compromised by several factors: unavailability – some or all parameters are unavailable for the area in question; unreliability – the parameters are not applicable for the area in question or are based on non-reliable and/or outdated observations; incompleteness – common for ridging parameters in general and resulting from the fact that they account only for ice ridges while all other deformed ice features not classified as ridges are disregarded.

Considering the above-mentioned issues in obtaining the reliable ridging parameters from databases, the goal of the present paper is to show the limitations of this approach and to present a novel method for calculating H_v when the ridging parameters are either unknown or unreliable. To the authors' knowledge, no method currently exists for calculating H_v that does not require some sort of ridging parameters as an input. The underlying idea behind the presented approach is that the amount of deformed ice can be associated with the thickness of ambient level ice. This idea has been long present in studies of shipping in ice and the correlation between level ice thicknesses and amount of ridging has been noticed amongst others by Kujala (1994), Romanov (1995) and Riska (1995). An issue with this approach is that ridging is a strongly stochastic feature, depending on

numerous other factors beside the level ice thickness, which can vary significantly from one location and season to another. However, the authors believe that for the practical purposes it is reasonable to establish area- and season-specific correlations between level ice thickness and equivalent-volume ice thickness. For this purpose, it is proposed that WMOITRs per SOD – currently accounting only for level ice thickness – are substituted with equivalent-volume ice thickness ranges (EVITRs), components of which represent one of the typical ice types (undeformed level ice, unconsolidated ice rubble from ridges, etc.). This in turn allows for the estimation of the total amount of ice, as well as its components, without the need for ridging parameters, and based only on the information available from the egg code for the area in question. It is considered by the authors that the idea of relating the equivalent-volume ice thickness to WMO SODs in this manner is novel. The procedure is developed to establish EVITRs based on the analysis of multiple datasets of underwater ice profiles for a certain area and season. Consequently, EVITRs in combination with egg code information on ice concentration and floe size can be used to calculate the amounts of different components of ice along the route. The presented methodology is tested on ice draft profiles obtained by submarine-based upward looking sonars (ULS) for several tracks in the Arctic.

The paper is structured as follows: in section 2, parameters of ice cover are described and terminology used in the rest of the paper is established. In section 3, H_v is calculated by traditional methods using egg code information combined with ridging parameters. The predicted amount of ice is compared to the actual one measured by a submarine-based ULS along several tracks in the Arctic. In section 4, the proposed methodology for developing EVITRs is presented. In section 5, the developed methodology is applied to available ULS-measured ice draft profiles and the results are compared to the traditional methods from section 3. Section 6 discusses the results and limitations of the presented methodology. Section 7 concludes the paper.

2. PARAMETERS OF ICE COVER

Ice field consists of ice floes defined as continuous ice pieces surrounded by open water, whose size can vary from order of meters to order of kilometers across (MANICE, 2005). Larger ice floes usually consist of level ice segments ("Level ice is a region of ice with relatively uniform thickness." ISO19906, 2010) formed through thermodynamic growth of ice thickness, in addition to areas of deformed ice (ice ridges, rafts and ice rubble) created due to mechanical forcing. According to NSIDC (2006) and MANICE (2005), level ice can also be called undeformed ice. In this paper, both terms are used interchangeably.

The coding system for WMO egg code classification used in the ice charts (WMO, 1970) is presented in Table 1, together with coding for SIGRID format (Thompson, 1981), which is often used in ice charts databases available on the Internet.

Table 1. System used for egg code classification (according to WMO and SIGRID)

Ice concentration (IC)			Stage of development of ice (SOD)				Ice form (IF)			
Definition	WMO code	SIGRID code	Definition	Ice thickness range (WMOITR)	WMO code	SIGRID code	Definition	Floe size (across)	WMO code	SIGRID code
Ice free	0	0	Ice free	-	0	0	Pancake ice	30 cm - 3 m	0	0
< 1/10	0	01	New ice	-	1	81	Shuga/ Brash ice	< 2 m	01	1
Bergy water	1	02	Nilas	< 10 cm	2	82	Ice cake	< 20 m	02	2
1/10th	1	10	Young ice	10 - 30 cm	3	83	Small floe	20 – 100 m	0	3
2/10th	2	20	Grey ice	10 - 15 cm	4	84	Medium floe	100 - 500 m	20	4
3/10th	3	30	Grey-white ice	15 - 30 cm	5	85	Big floe	500 m - 2 km	30	5
4/10th	4	40	First year ice	30 - 200 cm	6	86	Vast floe	2 km - 10 km	40	6
5/10th	5	50	Thin first year ice	30 - 70 cm	7	87	Giant floe	> 10 km	50	7
6/10th	6	60	Thin first year ice - stage 1	30 - 50 cm	8	88	Fast ice	-	60	8
7/10th	7	70	Thin first year ice - stage 2	50 - 70 cm	9	89	Growlers Floebergs	-	70	9
8/10th	8	80	Medium first year ice	70 - 120 cm	1.	91	Icebergs	-	80	10
9/10th	9	90	Thick first year ice	120 - 200 cm	4.	93				
9/10th - 10/10th	9+	91	Old ice	> 200 cm	7.	95				
10/10th	10	92	Second year ice	> 200 cm	8.	96				

Multi-year ice	> 200 cm	9.	97
Glacier ice	-	^.	98
Undetermined /Unknown	-	X	99

Morphology of a typical ice ridge is presented in Figure 1. Ridge consists of keel (h_k), being the part of ridge below the waterline, and sail (h_s), part of ridge above the waterline. Both keel and sail are assumed to have triangular cross section, with base angles equal to α_k and α_s. Keel consists of keel rubble (h_{kr}, which consists of thermally consolidated ice below parent level ice sheet and unconsolidated keel rubble), and underwater part of parent level ice sheet (keel lid). Sail consists of sail rubble (h_{sr}, which consists of thermally consolidated ice above parent level ice sheet and unconsolidated sail rubble), and freeboard part of parent level ice sheet (sail lid). Keel and sail have the same width equal to w_r. Consolidated layer (h_{cl}) is a part of ridge with no voids, and consists of thermally consolidated ice in ridge keel and sail, together with parent level ice sheet (keel and sail lids).

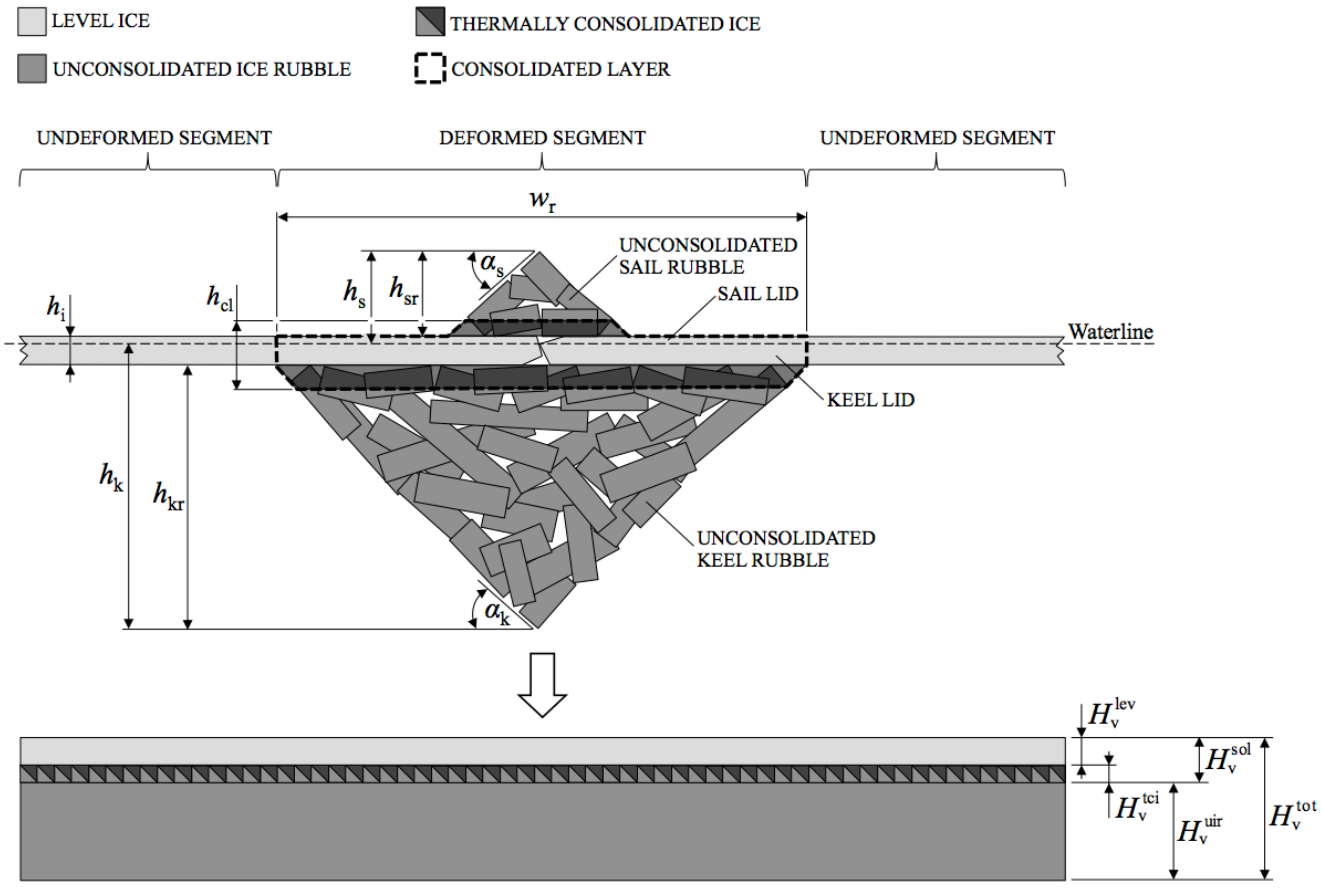

Figure 1. Ice profile morphology and illustration of concept of equivalent-volume ice thickness with its components

Figure 1 also shows a portion of a typical ice profile consisting of undeformed ice (or level ice, h_i) containing a deformed ice feature (ice ridge). Furthermore, logic of decomposition of actual ice profile into components of equivalent-volume ice thickness is presented. H_v is separated into several components according to Equation 1, which are:

- H_v^{lev} – Level ice component. Accounts both for level ice between the ridges and within the ridges' consolidated layer;
- H_v^{tci} – Thermally consolidated ice component. Accounts for thermally consolidated ice from ridge's consolidated layer, after the parent level ice has been subtracted;
- H_v^{sol} – Solid ice component. Accounts for all solid ice, which consists of level ice and thermally consolidated ice, according to Equation 2. Grouping these two together as solid ice is justified by the assumption that the ship resistance in thermally consolidated ice follows similar laws as that in level ice, as pointed out by Li et al. (2018);
- H_v^{uir} – Unconsolidated ice rubble component. Accounts for all unconsolidated ice rubble from ridge keel and sail and from other deformed features. Voids in ice rubble are excluded by applying the porosity factor.
- H_v^{tot} – Total equivalent-volume ice thickness. Represents all ice regardless of its origin (see Equation 3). When the cross sectional areal of equivalent-volume ice thickness profile is calculated using H_v^{tot}, it equals the cross sectional area of the original ice profile (excluding the porosity of ice rubble). By this definition, H_v^{tot} is similar to state of the art definitions of H_v as in Leppäranta (1980) and Riska (2010). It should be noted that the total amount of ice is strongly influenced by the assumed triangular shape of ridge keel and sail, which is a simplification of reality, but a necessary assumption.

$$H_v = \begin{bmatrix} H_v^{lev} \\ H_v^{tci} \\ H_v^{sol} \\ H_v^{uir} \\ H_v^{tot} \end{bmatrix} \quad \text{Eq. (1)}$$

$$H_v^{sol} = H_v^{lev} + H_v^{tci} \quad \text{Eq. (2)}$$

$$H_v^{tot} = H_v^{sol} + H_v^{uir} \quad \text{Eq. (3)}$$

The reason to separate H_v into components comes from the need to distinguish resistance in solid ice to that in unconsolidated ice rubble. This distinction is needed when calculating resistance of icebreakers and ice-going vessels[1], where the total resistance can be calculated by superimposing resistance in solid ice (function of H_v^{sol}) and resistance in unconsolidated ice rubble (function of H_v^{uir}). On the other hand, resistance of ice-strengthened vessels[2] depends on the ice volume in a channel following an icebreaker, regardless whether it comes from unconsolidated ice rubble or from solid ice. In this case, total resistance is a function of H_v^{tot}.

3. RIDGING PARAMETERS-BASED METHOD FOR THE CALCULATION OF EQUIVALENT-VOLUME ICE THICKNESS

In this section, traditional method for calculating equivalent-volume ice thickness is presented and used to determine the total amount of ice (*I*) expected along several tracks in the Arctic. The results are compared to the actual amount of ice detected along the same

[1] Ice-going vessels can break ice on their own and require icebreaker support only in heaviest ice conditions (Riska, 2010).
[2] Ice-strengthened vessels cannot break ice on their own. They can sail only in very light ice conditions independently, or through a brash ice channel created by an icebreaker (Riska, 2010).

tracks by the submarine-based ULS (I_{ULS}). Details about submarine ULS measurements and the exact procedure for the calculation of I_{ULS} are given in sections 4 and 5.

3.1 Egg code data for the tested tracks

Four tracks for which the calculations are done are shown in Figure 2 and are called tested tracks in further text. The egg code data (in SIGRID format) is acquired from the historical ice charts database developed by Tõns et al. (2014) for each tested track for the exact time and location where the submarines have done their measurements. Since the submarine tracks are divided in track segments of usually 50 km or less in length, the geographical center of each track segment is taken as a representative point for determining the egg code parameters for the track segment in question. This implies that the ice chart polygon, in which the geographical center of the track segment falls, is representative for the entire track segment. Given the usual length of track segments, this simplification should not affect the results significantly, as the egg code polygons for the high latitude tracks are considerably larger than the length of an average track segment. For each of the track segments of the tested track, egg code data in SIGRID format is preprocessed and transformed into readable parameters for ice concentration, stage of development and floe size, according to SIGRID coding system shown in Table 1.

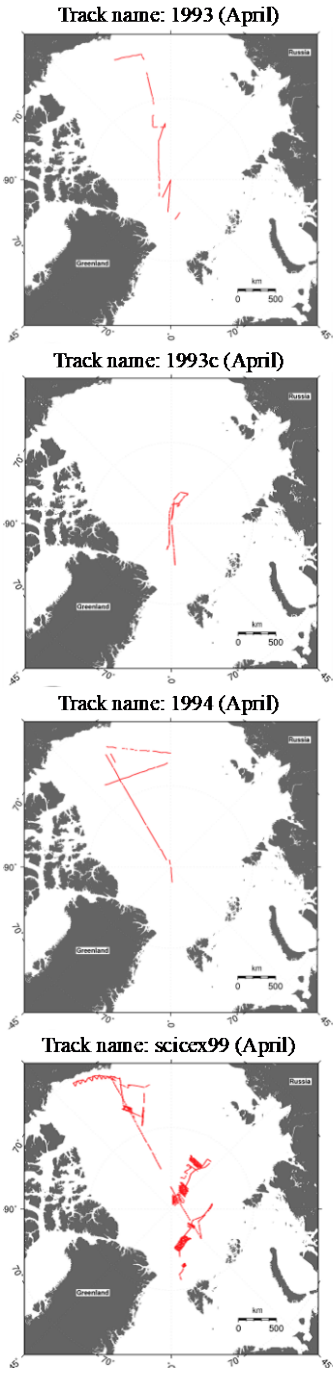

Figure 2. Geographical locations of tested submarine tracks (figure taken from NSIDC, 2006)

3.2 Ridging parameters

Since the tested tracks are located in the high Arctic, ridging parameters are not available as a supplement to the egg code. Therefore, they need to be estimated from a different source. Since the database developed by Romanov (1995) is the most comprehensive and widely used database of ridging parameters for the Arctic available, it is used in this study. Ridge density in number of ridges per unit of distance (μ) is given in form of an exponential probability distribution, which is in the Romanov's study assumed to be valid for the entire Arctic, and independent on the season, area, or SOD of ambient level ice. The average value of this parameter is 2 ridges/km, which is the value used in this paper. Ridge keel depth (h_k) is calculated by combining ratios of h_k/h_s and h_i/h_s, where h_i is obtained from the egg code. Ratios h_i/h_s are given in Romanov (1995) as area-specific values for different regions in the Arctic, and in this calculation obtain different values depending on the location of the tested track. h_k/h_s is set to 4.5 according to Wright et al. (1978).

3.3 Calculation of H_v and I

To establish a base case, equivalent-volume ice thickness is first calculated without the ridging parameters and based only on the level ice thickness obtained from WMOITRs. For this purpose, a procedure similar to the one presented in Schellenberg (2002) is used, based on which the Equation 4 is established. $H_{v_{WMO}}$ represents average level ice thickness of (usually) three predominant ice categories defined by the egg code for an ice chart polygon. $h_{i_{WMO}}$ is the level ice thickness obtained from WMOITR for each respective ice category (SOD). Since the WMOITR covers an entire range of ice thicknesses (e.g. 70-120 cm for Medium first year ice, see Table 1), and if there is no further information on distribution between those limits, usually the means of these ranges ($\bar{h}_{i_{WMO}}$) are used as representative values (according to Prinsenberg and Peterson, 2003 and Geiger, 2006). However, depending on the month, other values can be used. Since all tested tracks in this study have been recorded during the month of April, it is expected that the level ice thickness for higher SODs will be closer to the upper limit of the range during that period

of year. Therefore, the following values of $h_{i_{WMO}}$ are used: 1.2 m for Medium first year ice and 1.8 m for Thick first year ice and First year ice. For the lower SODs, $\bar{h}_{i_{WMO}}$ are used. $h_{i_{WMO}}$ for Multi-year ice could not be estimated based only on the WMO classification, since the upper limit of the range is missing, see Table 1. Therefore, for the purpose of this paper, $h_{i_{WMO}}$ is assumed to be 2.5 m for Multi-year ice (Riska, 2010). Old ice, Second year ice and Multi-year ice SODs are all treated as Multi-year ice. Note in Equations 4, 6 and 8 that H_v is calculated separately for each of the predominant ice categories (ic) in an area described by the egg code, which are then summed up and normalized by the total ice concentration (c_{tot}) to exclude the open water parts from the average ice thickness. Index *i* in those equations marks the value of the variable specific for the i-th ice category. Note that some variables, which have constant value in all iterations (e.g. μ in Equation 6), stand without ice category index. Number of ice categories (N_{ic}) from the egg code is usually three, but can be different.

$$H_{v_{WMO}} = \frac{\sum_{i=1}^{N_{ic}} h_{i_{WMO_i}} \cdot c_i}{c_{tot}} \qquad \text{Eq. (4)}$$

Consequently, knowing the length of each track segment (L_s) of the tested track, total amount of ice expected (I_{WMO}) considering only level ice can be calculated by summing up the amounts of ice in each track segment, according to Equation 5. Index *i* in Equations 5, 7 and 9 marks the value of the variable specific for the i-th track segment. N_s is a total number of track segments that the tested track consists of.

$$I_{WMO} = \sum_{i=1}^{N_s} H_{v_{WMO_i}} \cdot L_{s_i} \cdot c_{tot_i} \qquad \text{Eq. (5)}$$

In order to include also the deformed ice (ridges), procedure for the calculation of H_v given the ridging parameters is adopted from Riska (2010), based on which the Equation 6 is established (index rp stands for ridging parameters). Constants 4.28 and 2.14 in the equation assume a triangular ridge cross-section with α_k and α_s equal to 25°.

$$H_{v_{rp}} = \frac{\sum_{i=1}^{N_{ic}} h_{i_{WMO_i}} \cdot \left(c_i - 4.28 \cdot \mu \cdot h_{k_i}\right) + 2.14 \cdot \mu \cdot h_{k_i}^2}{c_{tot}} \quad \text{Eq. (6)}$$

Using the values of ridging parameters defined in section 3.2 (assuming they are constant for the entire area), and in combination with ice concentration and level ice thickness information for the tested track obtained from the egg code, it is possible to calculate the total amount of ice expected along the tested track taking both undeformed and deformed ice into account, according to Equation 7.

$$I_{rp} = \sum_{i=1}^{N_s} H_{v_{rp_i}} \cdot L_{s_i} \cdot c_{tot_i} \quad \text{Eq. (7)}$$

The results for the four tested tracks are summarized in Table 2. They show by how much percent the predicted amount of ice overshoots or undershoots the actual amount of ice detected by a submarine along the tested track.

Table 2. Traditional methods for calculation of total amount of ice along a tested track

Tested track	I_{WMO} (diff. to I_{ULS})	I_{rp} (diff. to I_{ULS})
1993 (April)	-34.7%	-30.0%
1993c (April)	-34.2%	-30.2%
1994 (April)	-33.8%	-29.1%
scicex99 (April)	-29.7%	-25.3%
Avg	-33.1%	-28.7%

It can be seen that the total amount of ice expected taking into account only level ice significantly underestimates the amount of ice detected by the submarines, by roughly 33% on average. This is expected, as it disregards the deformed ice features. When the ridges are added into the calculation, the expected amount of ice rises, but is still approximately 29% below the measured amount. This is an increase of only about 6% in the total amount of ice when the deformed ice is added, which is well below the values expected by Prinsenberg and Peterson (2003) who show the increase of the ice thickness due to

deformed ice of 20-80%. This indicates that the values of ridging parameters for the Arctic used in this study – even though coming from a widely used database – may not be sufficient for an accurate estimation of ice conditions.

4. METHODOLOGY FOR THE CALCULATION OF EQUIVALENT-VOLUME ICE THICKNESS RANGES

In this section, the methodology for the calculation of equivalent-volume ice thickness ranges (EVITRs) for different components of H_v is presented. It is proposed that the WMOITRs per SOD are substituted with area- and season-specific EVITRs, which could be used for the calculation of the amounts of different components of ice expected along a shipping route. EVITRs are established based on the analysis of underwater ice profile data.

An idealized example of part of underwater ice profile with ice draft measurements of undeformed and deformed segments (d_{und} and d_{def}) at 1 m spacing is shown in Figure 3.

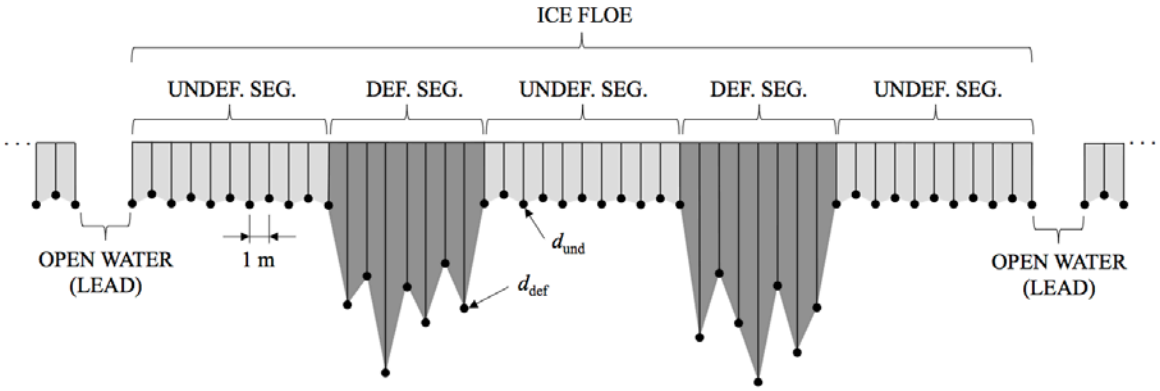

Figure 3. Idealized example of an ice draft profile

In order to determine EVITRs, a procedure is applied to a series of such ice draft profiles according to the following steps:

1) Identification of individual ice floes:

First, individual ice floes are identified from the ice draft profiles. This is done in order to exclude the open water parts from the calculation of floe's H_v, since this parameter is included in the calculations later through ice concentration obtained from the egg code.

Therefore, in order to identify single floes, leads or patches of open water between the floes are detected. The following principle found in NSIDC (2006) is used for identification of leads: "Leads are defined as a series of consecutive drafts, all of depth less than 0.3 m, that span a distance 10.0 m or greater in length." There is no clear distinction between leads (which may contain brash ice, nilas and/or young ice) and open water (fully free of ice) in the NSIDC interpretation. This is due to the fact that NSIDC data is based on ice profiles obtained by the submarine-based ULS, which are not accurate in measuring thinner drafts. Therefore, it is assumed that there is no difference between leads and open water. In other words, all ice thickness measurements identified as leads are set to zero, which results in disregarding all ice thinner than 30 cm. This limitation does not introduce an error in the context of the presented methodology, since the purpose of identification of leads/open water is solely to make a distinction between the neighboring ice floes. However, this assumption does result in underestimation of total amount of ice in the ice profile.

2) Identification of undeformed and deformed parts of an ice floe:

A typical ice floe can consist either of undeformed ice only or of a combination of undeformed and deformed ice (as in Figures 1 and 3). For each floe found using the procedure in step 1, undeformed and deformed parts of the floe need to be identified. The traditional approach for distinguishing between undeformed and deformed ice is to identify individual ice ridges (e.g. Timco and Burden, 1997; Strub-Klein and Sudom, 2012; Ekeberg, 2015), as they are the most significant deformed ice features. The remaining ice is then assumed to be undeformed. In the present study, the opposite approach is taken by identifying undeformed segments and considering all of the remaining ice to be deformed. For this purpose, four definitions of undeformed ice were found in the literature and tested for their applicability in the context of this study: the NSIDC (2006) definition (denoted as NSIDC below), two definitions from Wadhams and Horne (1980) (denoted as D1 and D2 in the original paper and also below), and another definition from Williams et al. (1975) (denoted as Williams below). Comparing the portions of undeformed ice detected using different definitions the following relations are noticed:

- D1 ≈ Williams
- D2 ≈ NSIDC

- D1 & Williams ≠ D2 & NSIDC

As can be seen from the above relations, the choice of the most appropriate definition of undeformed ice is reduced to choice between D1 and D2. As stated in the original paper and confirmed by testing in this study, D2 is more restrictive than D1: “D2 is not seeing all the level ice, but all that it sees is level ice.” In other words, using D2 disregards certain portions of level ice, while D1 results in false identification of some deformed ice features as level ice. Since in this study the level ice thickness is used to classify an ice floe per SOD from WMO classification, it is important that its accuracy is not compromised by inclusion of deformed ice features. Therefore, considering D2 ≈ NSIDC, definition of undeformed ice from NSIDC (2006) is used in this paper, which follows: "Undeformed ice is defined as a series of consecutive drafts, all of depth less than 5.0 m, that span a distance 10.0 m or greater in length over which the slope between adjacent drafts does not exceed 0.050. Deformed ice is all ice that is not classified as undeformed on the basis of these criteria."

3) Classification of ice floes and sub-floes per SOD:

After identifying the undeformed and deformed segments of an ice floe, each floe needs to be classified per WMO SOD. This is one of the main points of the presented method, as it will consequently allow assigning EVITRs to each SOD from the WMO classification. The reasoning follows from the fact that the SOD in the egg code is determined by the interpretation of SAR image, where a corresponding WMOITR (thickness range of undeformed ice) is associated to each SOD. Here, this logic is reversed, and by calculating the thickness of the undeformed ice, SOD per WMO classification is determined. For this purpose, average thickness of each undeformed segment within a floe is calculated. It is then checked to which of the WMO ice thickness ranges for different SODs from Table 1 it belongs, and a corresponding SOD category is assigned to the undeformed segment in question. E.g. if the average undeformed segment thickness is 40 cm, then its SOD is assigned as First year ice, Thin first year ice, and Thin first year ice – stage 1. As seen from the Table 1, some SOD categories contain sub-categories, thus the same undeformed segment can be assigned to more than one SOD category/sub-category, as in the example above.

Determining floe's SOD is more complicated, since assigning a single SOD to the entire floe is not always possible. This is especially the case with larger floes, which could be comprised of undeformed segments of different SODs. For this purpose, the following procedure is applied: if the total length of all undeformed segments with the same SOD (including the belonging deformed segments) spans over more than 90% of the floe's length, then the entire floe is assigned with the SOD in question. This is considered to be reasonable, as an ice floe mainly consisting of a single SOD will probably be classified with that SOD, regardless of possible inclusions of thinner or thicker undeformed ice, which might not even be detectable through SAR image analysis. Otherwise, if this condition is not met, the floe is separated into sub-floes each comprising of at least two consecutive undeformed segments of same SOD including the belonging deformed segments. If a sub-floe ends with a deformed segment followed by another sub-floe of different SOD, half of the deformed segment between the sub-floes is assigned to each of them. In the following steps, floes and sub-floes identified in this step are treated equally, and are called floes.

4) Calculation of components of equivalent-volume ice thickness for each floe:

Undeformed segments are considered to be in isostatic balance; thus, their draft measurements (d_{und}) are transformed into thicknesses considering the ice draft to be 93% of the ice thickness (Rothrock et al., 2008). With this information, total cross-sectional area of the floe's undeformed segments can be calculated.

On the other hand, deformed segments are more complicated to define since their complex structure needs to be deduced only from deformed draft measurements (d_{def}) and adjacent undeformed segments thicknesses. Here, several considerations are made:

- The area enveloped by deformed draft measurements represents deformed feature's keel, or the underwater part. In order to calculate the amount of ice above the waterline, the following relations from Timco and Burden (1997) are used: $A_k = 7.96 \cdot A_s$ for First-year ice, and $A_k = 8.81 \cdot A_s$ for Multi-year ice, where A_{k} is the enveloped keel area, and A_{s} is the enveloped sail area.

- If the SOD of the two adjacent undeformed segments is Multi-year ice, then the deformed feature between them is considered to be fully consolidated, according to Høyland et al. (2008).
- If the SOD of the two adjacent undeformed segments is First-year ice, then several options are possible. First, if the sum of enveloped areas of keel and sail (considering the A_k/A_s relations from above) is less than the area described by the average of two adjacent undeformed segments thicknesses and length of deformed segment, then the deformed segment is considered to be ice rubble since its area is insufficient to accommodate the ridge's consolidated layer of minimal thickness (minimal thickness means no thermal consolidation in ridge keel or sail). Ice rubble is considered to be pile of unconsolidated ice pieces with porosity (ρ) equal to 20% (according to Melling and Riedel, 1995). Conversely, if the deformed ice feature is large enough to accommodate the consolidated layer of minimal thickness, it is considered to be a ridge with consolidated layer equal to average ambient level ice thickness, with the rest of the ice being keel and sail unconsolidated rubble, with the same porosity of 20%. Finally, if the ridge is large enough to accommodate the fully grown consolidated layer of maximal thickness (1.75 times the average ambient level ice thickness, according to Høyland et al., 2008), then the thickness of consolidated layer is set to that value, with the same considerations for keel and sail unconsolidated rubble as for the smaller ridge.

Considering the points from above, cross-sectional areas of floe's components can be calculated: A_{lev}, A_{tci}, A_{sol}, A_{uir}, and A_{tot}, with indices having the same meaning as the components of H_v described in section 2 and Figure 1. Finally, the cross-sectional areas of floe's components are divided by floe length (L_f) in order to obtain values of H_v^{lev}, H_v^{tci}, H_v^{sol}, H_v^{uir}, and H_v^{tot} following the logic from Figure 1. This procedure is repeated for each floe.

5) Calculation of EVITRs:

Ultimately, based on a large number of floes detected and values of components of H_v calculated for each of them, histograms for each component of H_v for different SODs from WMO classification can be generated. These histograms represent the newly established EVITRs, one for each significant component, namely: $EVITR_{sol}$, $EVITR_{uir}$, and $EVITR_{tot}$. If based on a sufficient number of ice floes, the histograms can be considered as good approximations of probability distributions. Each probability distribution (EVITR) is then characterized by the mean value of its equivalent-volume ice thickness component, $\bar{H}_v$.

5. CASE STUDY

In this section, the presented methodology for the calculation of EVITRs is applied to ice draft profiles obtained by submarines in the Arctic using ULS technology. The resulting EVITRs are then used to predict the amount of ice along the tested tracks and the results are compared to the traditional methods presented in section 3.

5.1 Submarine-based ULS ice draft profiles in the Arctic

US and British submarines equipped with ULS have been collecting data about the underwater surface of Arctic ice since the 1970s. Submarine-based ULS ice draft profile data is publically available from the US National Snow and Ice Data Center (NSIDC, 2006). All together, there are 39 submarine tracks with ice draft profiles available, consisting of ice draft measurements at roughly 1 m spacing. The first track was recorded in 1975, and the last one in 2005. The geographical locations of the tracks are shown in Figure 4. The complete list of tracks can be found in Table A-1 in the Appendix together with the original name and month for each track. Numerous studies have used ice draft profiles obtained by submarines, mainly for geophysical applications, e.g. Williams et al. (1975) and Wadhams (1984). See Tucker and Ackley (1998) and Rothrock and Wensnahan (2007) for a discussion on the scientific use of this data and its limitations.

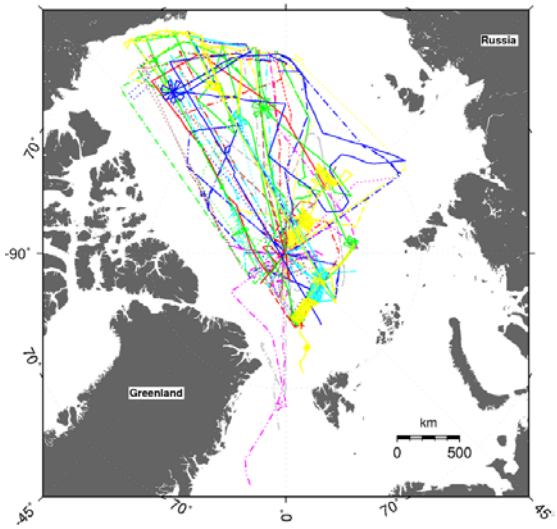

Figure 4. Geographical locations of available submarine tracks (figure taken from NSIDC, 2006)

5.2 Preprocessing of ice draft profiles

Each of the analyzed submarine tracks is divided into a number of track segments of typically 50 km in length containing ice draft measurements. The track segments can be shorter in cases where the measurements had to be stopped for different reasons. Draft measurements for each track segment are downloadable in the form of ASCII files, and can be in one of two different data formats**.** For data format 1, spacing between the adjacent drafts is explicitly given in the first column, with measured drafts in the second column. For data format 2, draft spacing is not explicitly given and thus is assumed to be constant and equal to 1 m, according to NSIDC (2006). In order to unify the draft spacing for all submarine tracks – which is necessary to keep the results consistent – draft profiles of tracks written in data format 1 are interpolated to 1 m draft spacing using linear interpolation. The interpolation procedure produces unrealistic drafts if the gap between two adjacent draft measurements is significantly larger than 1 m, which may result in artificial formation of nonexistent portions of level ice. Therefore, track segments written in data format 1 are split into separate sub-segments at draft measurements between which a gap larger than 10 m is detected. The gap threshold of 10 m is chosen since this is the smallest gap length specified for data format 2. Similarly, track segments written in data format 2 are split into sub-segments at draft measurements denoted in the file header. Each of these resulting sub-segments is then treated equally as a standard track segment.

5.3 Establishing EVITRs based on ice draft profiles

The EVITRs are established based on the analysis of ice draft profiles of several of the available 39 tracks. In order to select the tracks for building the nowadays-usable EVITRs, several considerations need to be made.

First, seasonality, which pertains to expected difference in EVITRs for the same SOD for different parts of the year. Here should be noted that only tracks recorded during freezing season are analyzed, since the WMO SODs are not representative for ice classification during melting season due to thawing processes. Seasonality is defined according to Romanov (1995), freezing season being from October to May, and melting season from June to September (see Table A-1 in Appendix for division of tracks by season). Considering that characteristics of ice cover vary significantly during the freezing season itself, it would be useful to increase the resolution and establish monthly or bimonthly specific EVITRs. Unfortunately, the available ULS data does not cover all freezing season months. Therefore, EVITRs are generated for two bimonthly groups for which the available amount of data is sufficient: October-November and April-May.

Second, since the 39 available submarine tracks cover the span from 1975 to 2005, it is considered that more recent measurements are more relevant for today's ice conditions. This is mainly due to a well-documented trend of decrease of ice thickness and extent in the Arctic during the last decades (e.g. IPCC, 2007), which could result in difference in EVITRs for the same SOD for different years/decades. However, it should be noted that the effect of ice thickness/extent decrease on the change of EVITRs for the same SOD is unclear. Nevertheless, in order to account for possible importance of this, submarine tracks recorded between 1992 and 2005 are taken into account for calculation of nowadays-usable EVITRs. Granted, this implies fairly unchanged conditions between 2005 and present, which is also questionable. 1992 is provisionally taken as a cut-off year in order to have a minimal amount of tracks needed to provide a sufficient sample size of ice floes for establishing reliable EVITRs.

Considering the points above, tracks for both bimonthly groups are selected. The tracks are listed in Table 3 together with the cumulative number of floes (both relative and

absolute) from all tracks in a group based on which the EVITRs are calculated. It is considered that number of ice floes shown in Table 3 presents a sufficiently large sample for a statistical analysis, for both groups. Also, it is visible that for Oct-Nov group, relative amounts of thinner SODs is larger than for the Apr-May group, while the opposite is valid for the thicker SODs. This is expected due to ice growing processes towards the end of the winter and supports the applicability of the presented method for SOD classification. It should be noted here that based on the discussion in section 4, at least one undeformed segment within a floe is required for the calculation of floe's equivalent-volume ice thickness. This disqualifies all floes shorter than 10 m from the analysis (since this is the shortest segment needed to define undeformed ice) and also the floes where for whichever reason no undeformed segments are found. However, it is shown that these account only for a small portion of ice profiles, from 2% to 4% for each track. Components of EVITRs for both groups are shown in Figures 5 and 6.

Table 3. Selected tracks for both bimonthly groups and number of ice floes used for calculation of EVITRs

Group	Submarine tracks	Number of floes per SOD							Total floes
		Thin first year ice	Medium first year ice	Thick first year ice	Multi-year ice	Thin first year ice-stage 1	Thin first year ice-stage 2	First year ice	
Oct-Nov	2000a 2005e	5472 (12%)	3868 (8%)	8180 (18%)	7971 (17%)	3445 (7%)	1423 (3%)	16389 (35%)	46748 (100%)
Apr-May	1992a grayling92 L2-92 1993 1993c 1994 scicex99	1258 (3%)	2111 (5%)	10216 (26%)	13279 (34%)	719 (2%)	546 (1%)	11481 (29%)	39610 (100%)

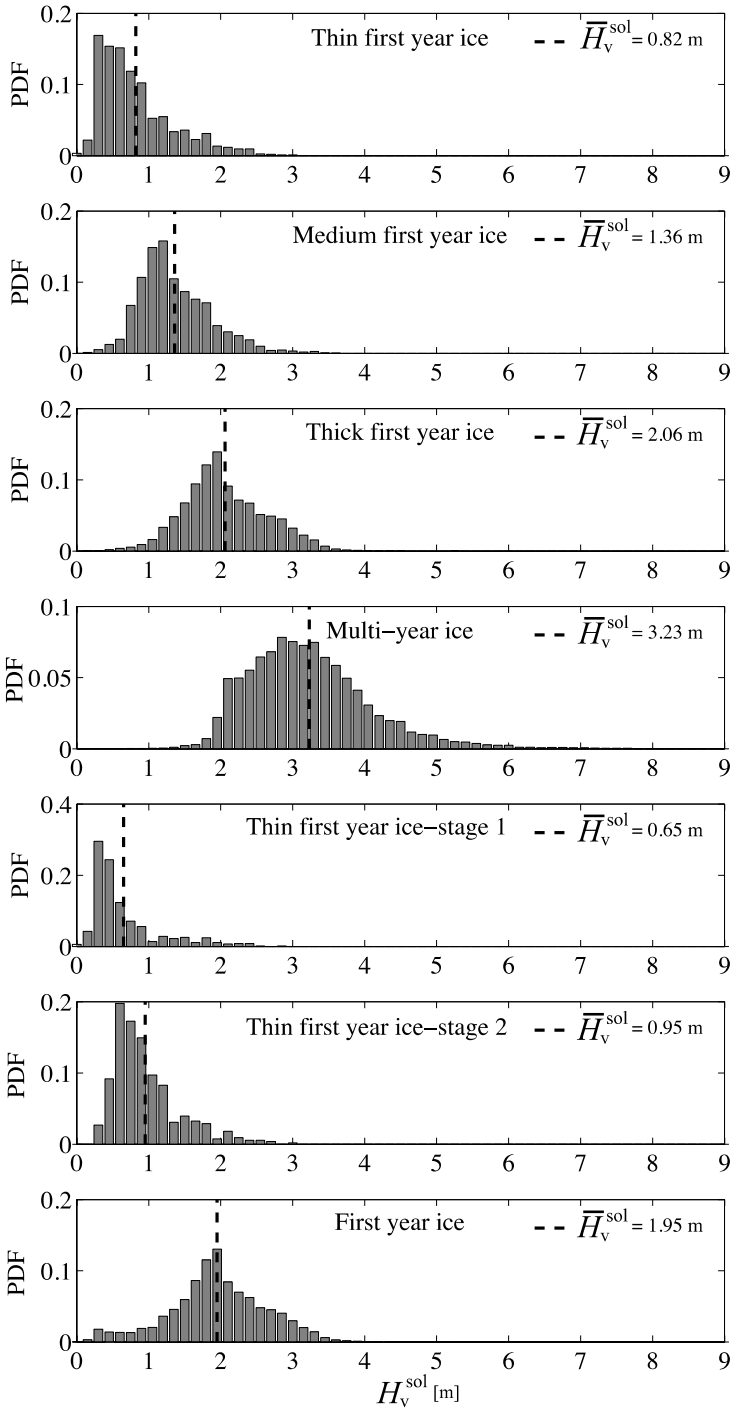

Figure 5a. $EVITR_{sol}$ for Apr-May group

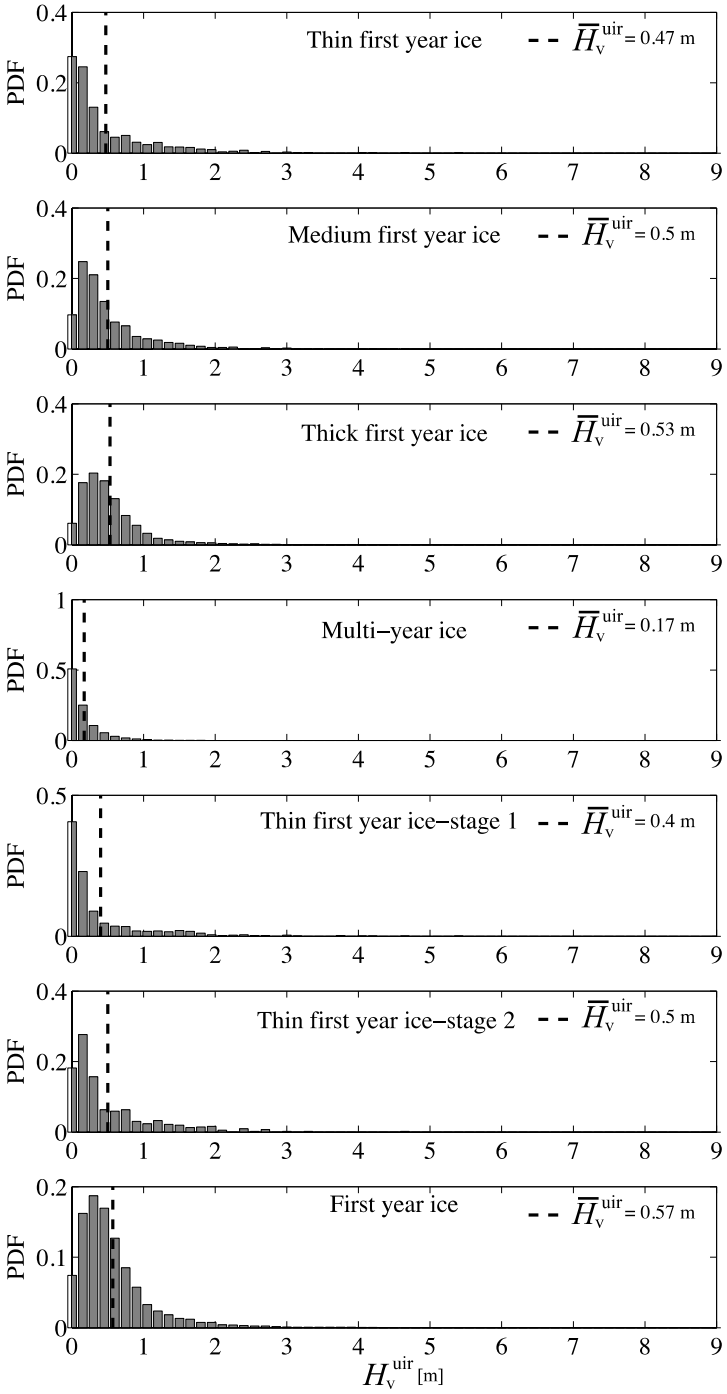

Figure 5b. EVITR$_{uir}$ for Apr-May group

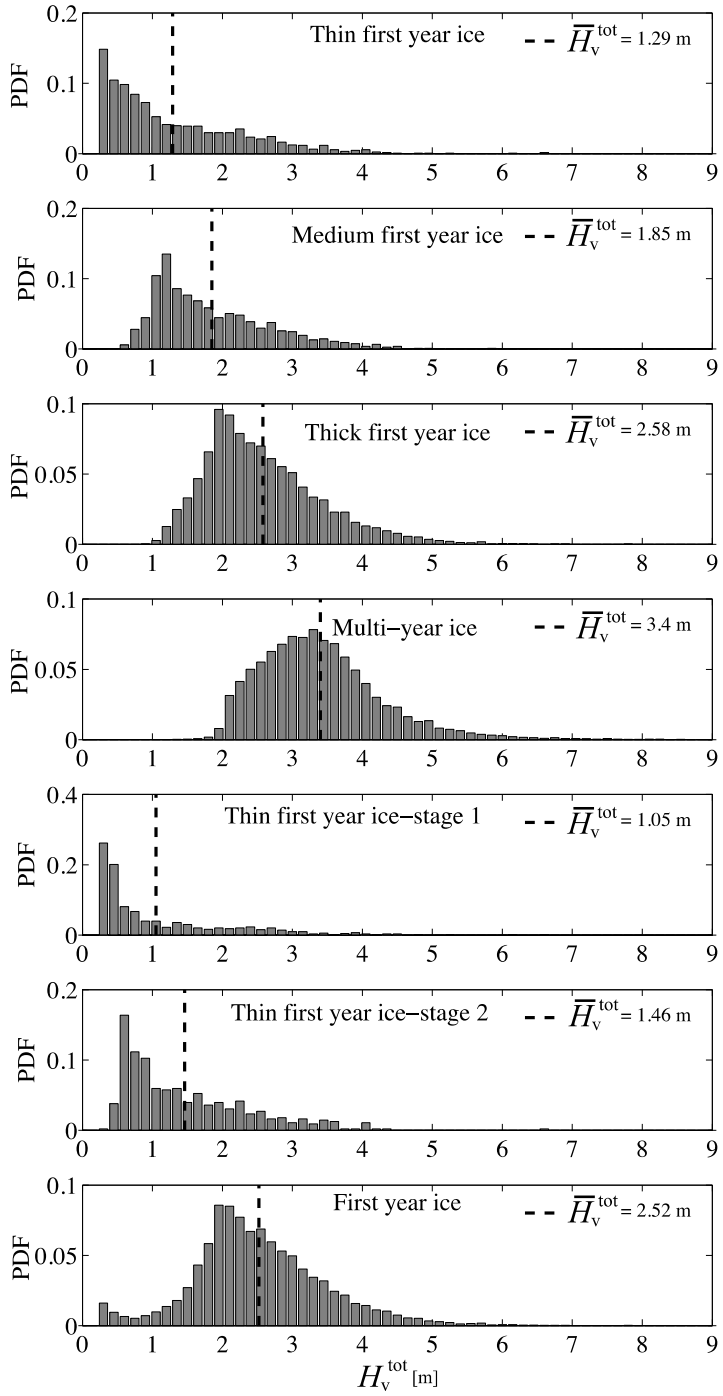

Figure 5c. $EVITR_{tot}$ for Apr-May group

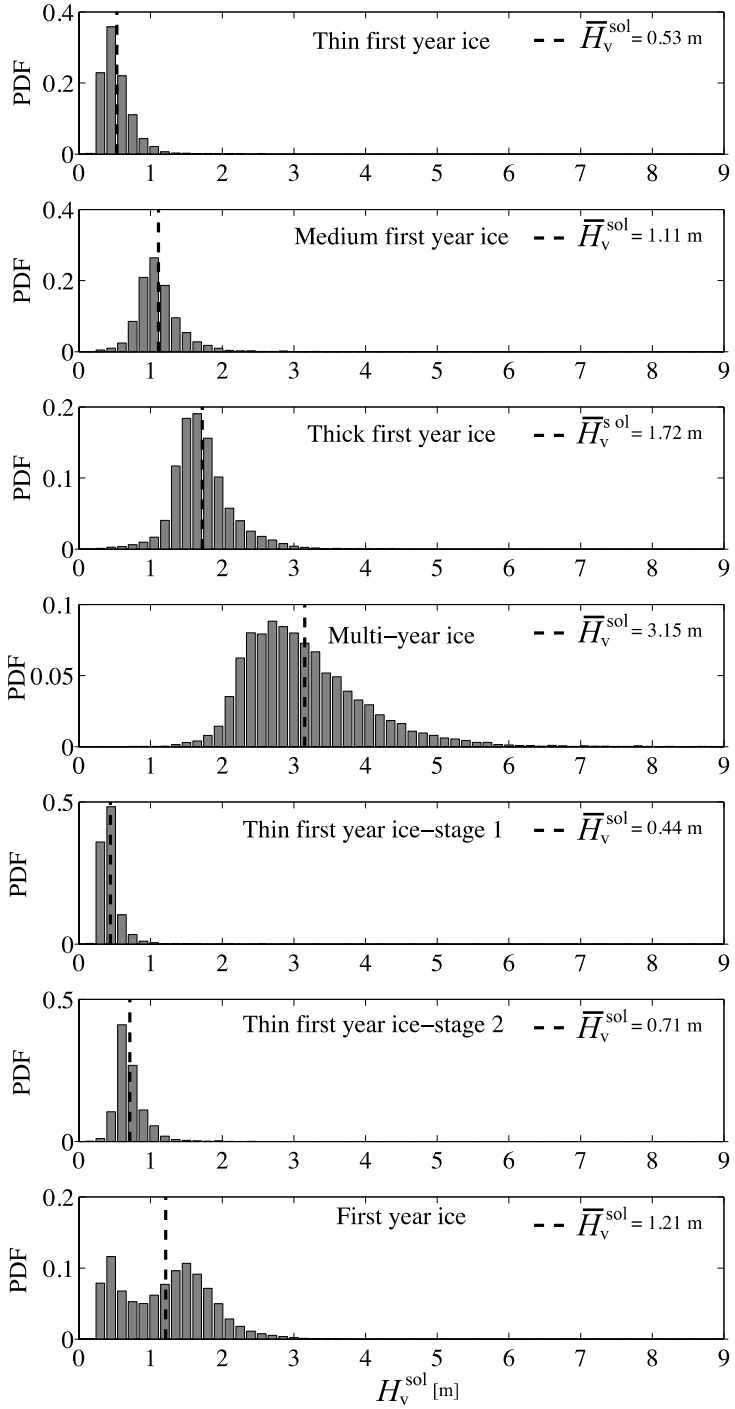

Figure 6a. $EVITR_{sol}$ for Oct-Nov group

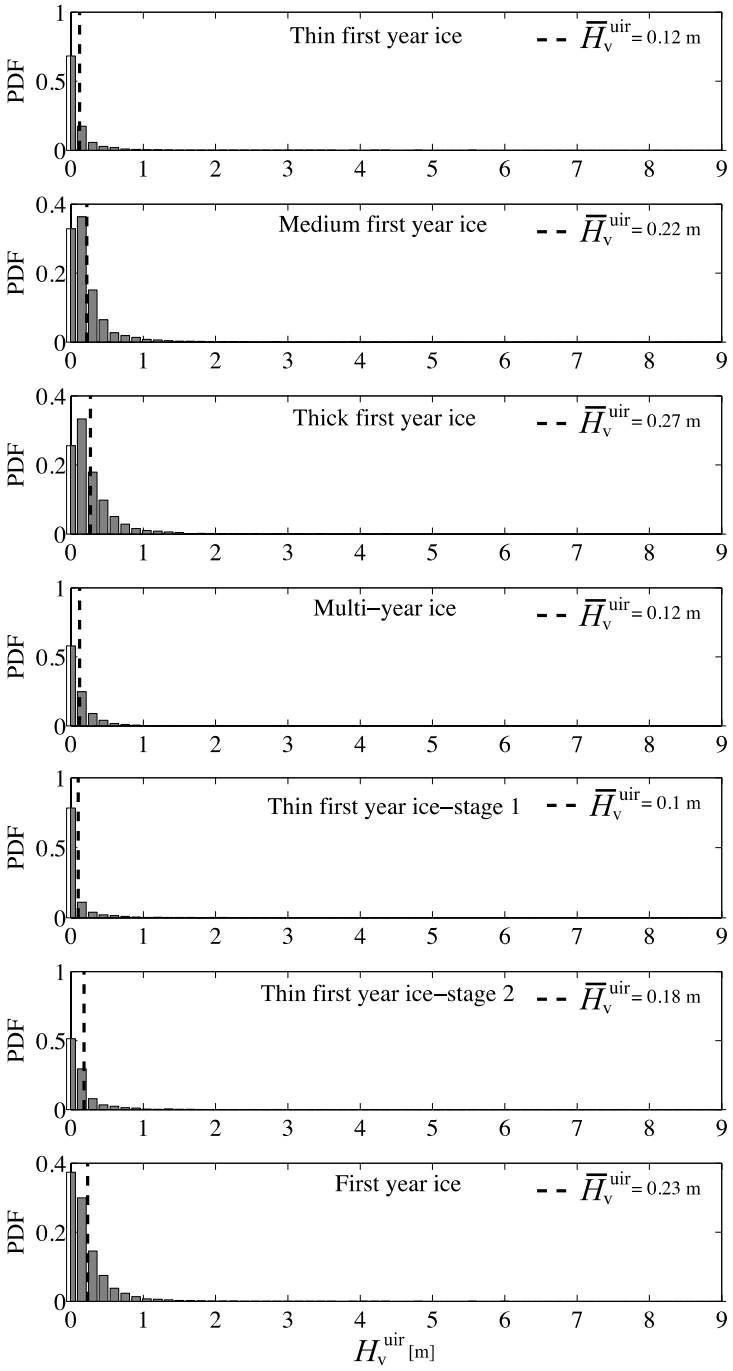

Figure 6b. EVITR$_{uir}$ for Oct-Nov group

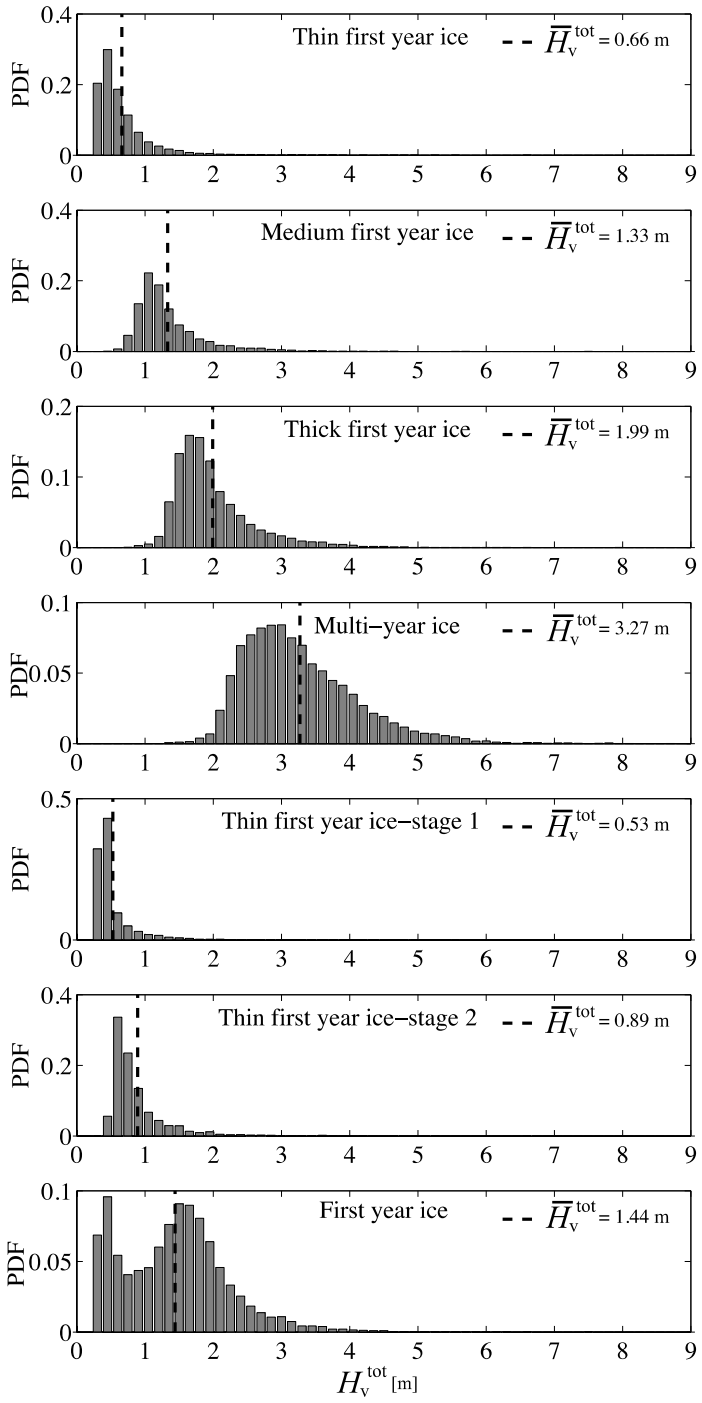

Figure 6c. $EVITR_{tot}$ for Oct-Nov group

The statistical analysis of the established $EVITR_{tot}$ is summarized in Table 4 and shown against WMOITRs where each SOD range is represented by its mean value, $\bar{h}_{i_{WMO}}$. For both groups, $EVITR_{tot}$ show increased average thickness compared to WMOITRs, which is expected since the deformed ice is added. The values are +34% on average for Oct-Nov group and +123% on average for Apr-May group. These results seem reasonable, since they are comparable to findings of Melling and Riedel (1995) and Prinsenberg and Peterson (2003). The difference is significantly higher for Apr-May group, which is also realistic considering the ice growth towards the end of winter.

Table 4. Statistical analysis of the established $EVITR_{tot}$

SOD	WMOITR [cm]	$\bar{h}_{i_{WMO}}$ [cm]	Oct-Nov group		Apr-May group	
			$\bar{H}_v^{tot}$ [cm]	$\frac{\bar{H}_v^{tot}}{\bar{h}_{i_{WMO}}}$	$\bar{H}_v^{tot}$ [cm]	$\frac{\bar{H}_v^{tot}}{\bar{h}_{i_{WMO}}}$
Nilas	<10	5	-	-	-	-
Young ice	(10, 30)	20	-	-	-	-
Grey ice	(10, 15)	12.5	-	-	-	-
Grey-white ice	(15, 30)	22.5	-	-	-	-
Thin first year ice	(30, 70)	50	66	+32%	129	+158%
Medium first year ice	(70, 120)	95	133	+40%	185	+95%
Thick first year ice	(120, 200)	160	199	+24%	258	+61%
Multi-year ice	>200	-	327	-	340	-
Thin first year ice-stage 1	(30, 50)	40	53	+32%	105	+160%
Thin first year ice-stage 2	(50, 70)	60	89	+48%	146	+143%
First year ice	(30, 200)	115	144	+25%	252	+119%
			Avg	+34%	Avg	+123%

5.4 Comparison with the ridging parameters-based method

The presented methodology for calculating the EVITRs is used to calculate the total amount of ice (I_{EVITR}) expected along the tested tracks from section 3. The actual amount of ice measured by submarines (I_{ULS}) is calculated as a total cross-sectional area of ice thickness profile, following the procedure from point 4 in section 4.

In the process of calculating I_{EVITR}, the first step is to determine the appropriate EVITRs applicable for each of the tested tracks. Note that $EVITR_{tot}$ are used here, since the comparison is made with methods preserving total ice volume presented in section 3, which do not make difference between different components of ice. To calculate $EVITR_{tot}$, 5 temporally nearest tracks of the same season recorded before the tested track are chosen. The tested track is excluded from this sample to avoid self-correlation. The number of 5 tracks is chosen as it is shown to provide a large enough sample for calculation of $EVITR_{tot}$, at the same time accounting for the specificity of the ice conditions in the Arctic at the time when the tested track was recorded. Once the appropriate $EVITR_{tot}$ are determined, a procedure similar to the one presented in Equation 4 is used to calculate the total equivalent–volume ice thickness for a tested track segment, see Equation 8.

$$H_v^{tot} = \frac{\sum_{i=1}^{N_{ic}} \bar{H}_{v_i}^{tot} \cdot c_i}{c_{tot}} \qquad \text{Eq. (8)}$$

It should be noted that when calculating H_v^{tot} in a case of occurrence of ice categories for which EVITR does not exist, instead of $\bar{H}_v^{tot}$, $\bar{h}_{i_{WMO}}$ are used. Also, the ice form parameter from the egg code is taken into account so that if the ice form for a certain ice category is smaller than Small floe (see Table 1), then $\bar{h}_{i_{WMO}}$ is used instead of $\bar{H}_v^{tot}$ even if the $EVITR_{tot}$ for this ice category exists. Reason for this is that an ice floe needs to be of sufficient size to accomodate both undeformed and deformed parts, while if it is smaller than Small floe, it is considered here to consist only of undeformed ice. Finally, I_{EVITR} for each tested track is calculated according to Equation 9.

$$I_{EVITR} = \sum_{i=1}^{N_s} H_{v_i}^{tot} \cdot L_{s_i} \cdot c_{tot_i} \quad \text{Eq. (9)}$$

The results from Table 2 are repeated and a column with I_{EVITR} is added, creating Table 5. It can be seen that using the method developed in this paper, expected amount of ice along the tested tracks is estimated more accurately compared to traditional methods using the currently available ridging parameters for the Arctic.

Table 5. EVITR-based method vs traditional methods for calculation of total amount of ice along a tested track

Tested track	I_{WMO} (diff. to I_{ULS})	I_{rp} (diff. to I_{ULS})	I_{EVITR} (% diff. to I_{ULS})
1993 (April)	-34.7%	-30.0%	+0.6
1993c (April)	-34.2%	-30.2%	+0.6
1994 (April)	-33.8%	-29.1%	-6.1
scicex99 (April)	-29.7%	-25.3%	-1.5
Avg	-33.1%	-28.7%	2.2% (abs)

6. DISCUSSION AND LIMITATIONS

Relating the equivalent-volume ice thickness solely to SOD is one of the basic assumptions of this study, which results in avoiding the need for ridging parameters. However, it is well known that ridging is a highly stochastic process depending on numerous parameters, which are difficult to simulate and predict. Nevertheless, the authors believe that the methodology presented in this paper can be used given a reliable and comprehensive dataset of ice profile measurements, and that the area- and season-specific EVITRs can be established for the practical use. Here it should be stated that the intention of the presented methodology is not to substitute the currently available methods using ridging parameters, but merely to offer an alternative in a case when the ridging parameters are unknown on unreliable.

The dataset on which the presented methodology is tested is not ideal for shipping purposes since it covers the high-latitude areas far from the regions of present human activities in the Arctic, which is closer to the shoreline. However, this is an unavoidable

limitation since these are the only tracks for which all parameters needed for the calculations were obtainable: egg code information, ridging parameters and submarine measurements. Therefore, it should be made clear that the EVITRs in Figures 5 and 6 are applicable only for the areas in the high Arctic, and should therefore be used with caution elsewhere. Also, they may not be fully representative for thinner SODs since the analyzed areas are predominantly covered with thicker ice categories. Furthermore, the accuracy of submarine-based ULS measurements is debatable, as discussed in Rothrock and Wensnahan (2007), especially for disregarding the ice thinner than 30 cm, which results in an underestimation of the actual amount of ice. However, since the submarines measure the underwater portion of the ice profile, which constitutes the majority of its thickness, it is considered that these measurements are superior to the ones taken from air or from satellites, which measure ice freeboard.

EVITRs in Figures 5 and 6 are not calculated for SODs where ice is thinner than 30 cm for the reasons stated above. However, given a reliable dataset of ice thickness measurements, EVITRs should also be established for thinner SODs since they can contain substantial amount of deformed ice.

The amounts of ice predicted by the traditional methods presented in Table 2 are largely influenced by the thickness of Multi-year ice, since this is a predominant SOD for the areas where the tested tracks were recorded. As noted earlier, this value is taken as 2.5 m, following the reasoning from Riska (2010). There is no consensus in the literature on this value (also the reason why it is not given in the WMO classification), thus this is a questionable assumption. However, as the maximal thickness of level ice per NSIDC (2006) definition is 5 m, and with lower limit of WMOITR for Multi-year ice being 2 m, 2.5 m taken as a representative value of this range seems to be reasonable, since any larger value than 2.5 m does not seem to be justified by the literature. In any case, noticed insufficient relative increase in the total amount of ice when the ridging parameters are added is independent of this value, supporting the conclusions about questionable applicability of available ridging parameters for the Arctic. Moreover, the Equation 6 from Riska (2010) does not take the porosity of ridge keels into account, but considers them to be solid blocks of ice. This is somewhat compensated by the fact that the equation does not

take ridge sails into account either. However, the effect of these two simplifications to the total ice balance is not clear.

Definitions of open water, level ice, and deformed ice used in this paper – although based on thorough literature review – are discussable since they influence the results significantly, and could be substituted if better and more reliable definitions become available. Nevertheless, approach taken in this paper pertaining to detection of level ice considering the remaining ice to be deformed, instead of identifying the individual ridges, is considered to be useful. The reason for this is twofold: first, to avoid choosing between numerous available criteria for detection of ice ridges; and second, with this approach, also other deformed ice features in addition to ridges are taken into account, which would have otherwise been neglected.

Probability distributions representing EVITRs for different SODs presented in Figures 5 and 6 are seen to have fairly large variance. This is accounted to several reasons. First, classification of ice floes per SOD cannot be done with complete accuracy, mainly due to uncertainty in accuracy of the submarine measurements. Second, submarines are following a line-like path underneath the ice, which for the purpose of characterization of two-dimensional ice field inherently introduces an error. Example of an idealized ice field is illustrated in Figure 7.

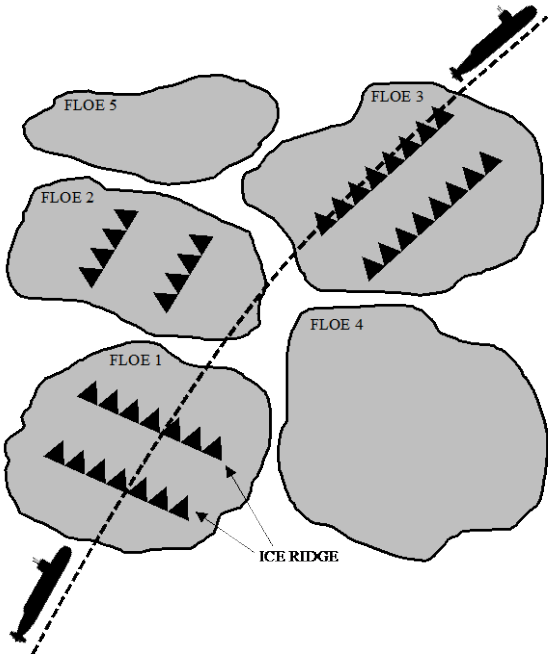

Figure 7. Example of an idealized ice field

Assuming floes 1-3 having the same SOD, it becomes obvious how a submarine may theoretically measure significantly different values of equivalent-volume ice thickness for the ice floes of same SOD, depending whether it travels perpendicularly to the ridge direction (as in floe 1), not detecting ridges at all (as in floe 2), or traveling along ridge direction (as in floe 3). However, considering the fact that EVITRs should be calculated based on a large sample of ice floes, these effects are assumed to be smeared into the average. Thus, mean values of EVITRs are considered to be representative, despite large variance. Also, it can be seen that some of the probability distributions are significantly skewed to one side, for which mode could be a more appropriate statistical characteristic than mean, but this is left for the users of the data to decide.

Large variance of EVITRs is further analyzed by examining the dependency between floes' H_v^{tot} and their lengths (L_f). Such analysis for SOD First year ice of April-May group is presented in Figure 8.

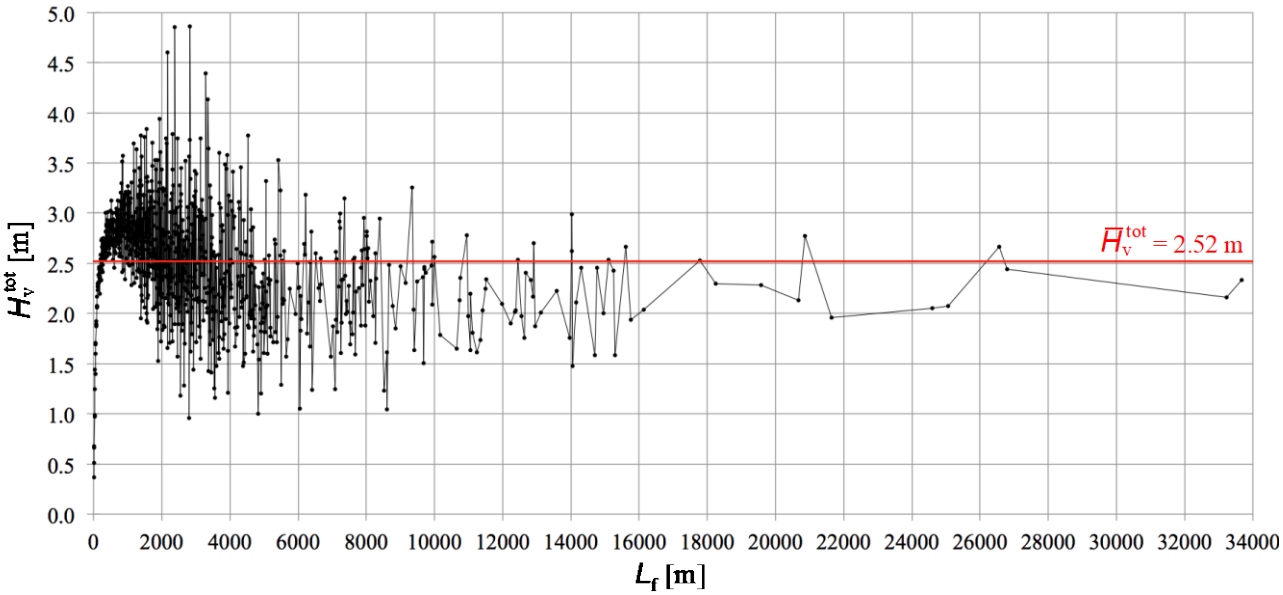

Figure 8. H_v^{tot} against floe length for First year ice of April-May group

Each point in the graph represents a mean value of H_v^{tot} for an L_f bin of 5 m. This means that the first point in the graph represents an average value of H_v^{tot} of all floes having length between 10 m and 15 m, second point represents floes having length between 15 m and 20 m, etc. Also, average H_v^{tot} of all floes is marked with red line. Some interesting patterns

can be noticed: H_v^{tot} of shorter floes starts from the lower limit of WMOITR for the SOD in question, and increases surprisingly regularly towards the average value. This is, however, considered to be reasonable, since floes need to be of certain size to accommodate significant amount of deformed features, which considerably contribute to H_v^{tot}. Also, as the floe length increases (largest floe found is almost 34 km long), it seems that H_v^{tot} moves closer to the average value. Note that the results shown in Figure 8 are for First year ice of Apr-May group, but similar pattern has been found also for other SODs and for Oct-Nov group.

7. CONCLUSIONS

In this paper, a novel method for estimation of the equivalent-volume ice thickness along vessel's sailing route through ice-covered waters is presented. The method does not require ridging parameters as an input, which makes it unique in the current state of the art.

The limitations of the currently available methods using ridging parameters are presented, showing underestimation of the expected amount of ice compared to the actual amount measured by the submarine-based ULS. Therefore, an alternative methodology for calculation of equivalent-volume ice thickness is presented. It is proposed that based on the analysis of the ice thickness profiles, standard WMO ice thickness ranges are substituted with newly developed equivalent-volume ice thickness ranges (EVITRs). The proposed methodology is tested on the ice draft profiles obtained by the submarines in the Arctic, showing a significant increase in accuracy compared to traditional methods. Therefore, the authors believe that the EVITR-based method presented in this paper can be of practical use, especially considering the limitations of the traditional approaches shown.

For the future work, the presented methodology could be used on a more reliable dataset of ice thickness measurements if such is, or becomes, available. This in not limited only to submarine-based ULS, but also autonomous underwater vehicles, helicopter-borne electromagnetic induction sensors, and other methods for accurate measurement of ice thickness could be used. Preferably, area- and season-specific datasets of ice thickness measurements could be analyzed, and a map of EVITRs for all SODs for different seasons

could be constructed for the entire Arctic basin, and possibly also for other ice-covered seas around the world.

Acknowledgements

The financial support by the Barents 2020 project (NOR-13/0080) funded by Norwegian Ministry of Foreign Affairs, as well as the support from the project partners, namely: ABB, CHNL, DNV GL, HiÅ (now part of NTNU), Marintek (now part of SINTEF Oceans), Northenergy and NTNU, are greatly appreciated. We also thank Mikko Lensu for valuable advices related to ice cover morphology.

APPENDIX

Table A-1. Submarine tracks available at NSIDC (2006) (superscript F for freezing season, M for melting season)

Track no.	Track name	Month
1.	1975	May^{F}
2.	1976	April^{F}
3.	UK76	April^{F}
4.	1979	April^{F}
5.	1981	October^{F}
6.	1982a	November^{F}
7.	1983a	August^{M}
8.	1984b	September^{M}
9.	1984c	November^{F}
10.	1984d	November^{F}
11.	1986a	May^{F}
12.	1986b	April^{F}
13.	1987	April^{F}
14.	1987c	June^{M}

15.	UK87	May[F]
16.	1988a	May[F]
17.	1988b	August[M]
18.	1988c	May[F]
19.	1989b	September[M]
20.	1990	March[F]
21.	1990c	September[M]
22.	1991	March-May[F]
23.	UK91	April[F]
24.	1992a	May[F]
25.	1992b	September[M]
26.	grayling92	April[F]
27.	L2-92	April[F]
28.	1993	April[F]
29.	1993c	April[F]
30.	scicex93	September[M]
31.	1994	April[F]
32.	1994b	September[M]
33.	scicex96_rev	September[M]
34.	scicex97_reproc	September[M]
35.	scicex98_rev	August[M]
36.	scicex99	April[F]
37.	2000a	October[F]
38.	2005a	July[M]
39.	2005e	November[F]

List of abbreviations

EVITR	Equivalent-volume ice thickness range
$EVITR_{sol}$	EVITR of solid component of H_v [m]
$EVITR_{tot}$	EVITR of total equivalent-volume ice thickness [m]
$EVITR_{uir}$	EVITR of unconsolidated ice rubble component of H_v [m]
ic	Ice category
NSIDC	National Snow and Ice Data Center
rp	Ridging parameters
SAR	Synthetic aperture radar
SOD	Stage of development of ice defined by WMO
ULS	Upward looking sonar
WMO	World Meteorological Organization
WMOITR	World Meteorological Organization ice thickness range

List of symbols

A_k	Ridge keel cross-sectional area [m^2]
A_{lev}	Cross-sectional area of floe's level ice [m^2]
A_s	Ridge sail cross-sectional area [m^2]
A_{sol}	Cross-sectional area of floe's solid ice [m^2]
A_{tci}	Cross-sectional area of floe's thermally consolidated ice [m^2]
A_{tot}	Total cross-sectional area of a floe [m^2]
A_{uir}	Cross-sectional area of floe's unconsolidated ice rubble [m^2]
c	Concentration of an ice category in an area [%]
c_{tot}	Total ice concentration in an area [%]
d_{und}	Ice draft measurement, undeformed ice [m]
d_{def}	Ice draft measurement, deformed ice [m]
H	Equivalent ice thickness [m]
H_p	Equivalent-performance ice thickness [m]
H_v	Equivalent-volume ice thickness [m]

H_v^{lev}	Level ice component of H_v [m]
H_v^{sol}	Solid ice component of H_v [m]
$\bar{H}_v^{sol}$	Mean value of $EVITR_{sol}$ [m]
H_v^{tci}	Thermally consolidated ice component of H_v [m]
H_v^{tot}	Total equivalent-volume ice thickness [m]
$\bar{H}_v^{tot}$	Mean value of $EVITR_{tot}$ [m]
H_v^{uir}	Unconsolidated ice rubble component of H_v [m]
$\bar{H}_v^{uir}$	Mean value of $EVITR_{uir}$ [m]
$H_{v_{WMO}}$	H_v considering only level ice from WMO classification [m]
$H_{v_{rp}}$	H_v with ridging parameters describing the deformed ice [m]
h_{cl}	Thickness of ridge consolidated layer [m]
h_i	Level ice thickness [m]
$h_{i_{WMO}}$	Level ice thickness from WMOITR [m]
$\bar{h}_{i_{WMO}}$	Mean value of WMOITR [m]
h_k	Depth of ridge keel [m]
h_{kr}	Depth of ridge keel rubble [m]
h_s	Height of ridge sail [m]
h_{sr}	Height of ridge sail rubble [m]
i	Iteration index denoting either ice category or track segment [-]
I	Total amount of ice detected/calculated along certain track [m^2]
I_{EVITR}	I based on mean values of $EVITR_{tot}$ [m^2]
I_{rp}	I considering level ice and ridging parameters [m^2]
I_{ULS}	I detected by submarine-based ULS [m^2]
I_{WMO}	I considering only level ice from WMO classification [m^2]
L_f	Floe length [m]
L_s	Length of a single submarine track segment [m]
N_{ic}	Number of egg code ice categories in an area [-]
N_s	Number of segments a tested submarine track consists of [-]
w_r	Ridge width [m]
α_k	Base angle of ridge keel [deg]

α_s Base angle of ridge sail [deg]

μ Ridge density in number of ridges per unit of distance [1/m]

ρ Ice rubble porosity [-]

REFERENCES

Bergström, M., Erikstad, S.O., Ehlers, S., 2016. A simulation-based probabilistic design method for arctic sea transport systems. Journal of Marine Science and Application, Vol. 15, pp. 349-369.

Bertoia, C., Manore, M., Steen Andersen, H., O'Connors, C., Hansen, K.Q., Evanego, C, 2004. Synthetic aperture radar for operational ice observation and analysis, in: Jackson, C.R., Apel, J.R. (Eds.), Synthetic Aperture Radar Marine User's Manual. National Oceanic and Atmospheric Administration, Washington D.C., pp. 417-442.

Ekeberg, O.C., 2015. Studies of Ice Ridge Shape and Geometry from Upward Looking Sonar Data. (Doctoral Thesis) Norwegian University of Science and Technology, Trondheim.

Geiger, C.A., 2006. Propagation of Uncertainties in Sea Ice Thickness Calculations from Basin-Scale Operational Observations. Cold Regions Research and Engineering Laboratory, U.S. Army Engineer Research and Development Center, Hanover.

Høyland, K.V., Barrault, S., Gerland, S., Goodwin, H., Nicolaus, M., Olsen, O.M., Rinne, E., 2008. The consolidation in second and multiyear sea ice ridges Part 1: Measurements in early winter. 19th IAHR International Symposium on Ice, Vancouver, Canada, pp. 1231-1241.

IPCC, 2007. Climate Change 2007: Impacts, Adaptation and Vulnerability, in: Parry. M.L., Canziani, O.F., Palutikof, J.P., van der Linden, P.J., Hanson, C.E., (Eds.), Contribution of Working Group II to the Fourth Assessment Report of the Intergovernmental Panel on Climate Change. Cambridge University Press, Cambridge, pp. 976.

ISO19906, 2010. Petroleum and natural gas industries - Arctic offshore structures, International Standard, International Standardization Organization, Geneva.

Kujala, P., 1994. On the Statistics of Ice Loads on Ship Hulls in the Baltic. Acta Polytech. Scandinavica, Rpt Me 116, Helsinki, 98 p.

Kuuliala, L., Kujala, P., Suominen, M., Montewka, J., 2017. Estimating operability of ships in ridged ice fields. Cold Reg. Sci. Technol., 135 (2017), pp. 51-61.

Leppäranta, M., 1980. On the Drift and Deformation of the Sea Ice Fields in the Bothnian Bay. Finnish Maritime Administration: Tech. rep., Winter Navigation Research Board. Res. Rpt. 29, 79 p.

Li, F., Goerlandt, F., Kujala, P., Lehtiranta, J., Lensu, M., 2018. Evaluation of selected state-of-the-art methods for ship transit simulation in various ice conditions based on full-scale measurement. Cold Reg. Sci. Technol., 151 (2018), pp. 94-108.

MANICE, 2005. Manual of Standard Procedures for Observing and Reporting Ice Conditions. Canadian Ice Service, ISBN 0-660-62858-9.

Melling, H., Riedel, D.A., 1995. The underside topography of sea ice over the continental shelf of the Beaufort Sea in the winter of 1990. Journal of Geophysical Research. 100(C7):13641-13653.

NSIDC, 2006. National Snow and Ice Data Center (comp.). 1998, updated 2006. Submarine Upward Looking Sonar Ice Draft Profile Data and Statistics, Version 1. Boulder, Colorado USA. NSIDC: National Snow and Ice Data Center. doi: https://doi.org/10.7265/N54Q7RWK. (accessed 4.3.18).

Prinsenberg, S.J., Peterson, I.K., 2003. Comparing ice chart parameters against ice observations. Proceedings of the 13th Int. Offshore and Polar Eng. Conf, Honolulu. Vol. 1, 733-738.

Riska, K., 1995. Ice conditions along the north-east passage in view of ship trafficability studies. Proc. 5th International Offshore and Polar Engineering Conference, The Hague. II, 420-427.

Riska, K., 2009. Definition of the new ice class 1A Super+. Finnish Maritime Administration: Tech. rep., Winter Navigation Research Board. Res. Rpt. 60.

Riska, K., 2010. Ship–Ice Interaction in Ship Design: Theory and Practice. Encyclopedia of Life Support Systems (EOLSS), Paris.

Romanov, I.P., 1995. Atlas of Ice and Snow of the Arctic Basin and Siberian Shelf Seas. Backbone Publishing Company.

Rothrock, D.A., Wensnahan, M., 2007. The accuracy of sea ice drafts measured from U.S. Navy submarines. Journal of Atmospheric and Oceanic Technology. 24 (11): 1936-49. DOI: 10.1175/JTECH2097.1.

Rothrock, D.A., Percival, D.B., Wensnahan, M., 2008. The decline in arctic sea-ice thickness: Separating the spatial, annual, and interannual variability in a quarter century of submarine data. J. Geophys. Res. 113, C05003, DOI:10.1029/2007JC004252.

Sandven, S., Johannessen, O.M., Kloster, K., 2006. Sea ice monitoring by remote sensing. Encyclopedia of Analytical Chemistry. DOI: 10.1002/9780470027318.a2320.

Schellenberg, B., 2002. Investigation of Sea-Ice Thickness Variability in the Ross Sea. (Master's Thesis) University of Delaware.

Strub-Klein, L., Sudom, D., 2012. A comprehensive analysis of the morphology of first-year sea ice ridges. Cold Reg. Sci. Technol., 82 (2012), pp. 94-109. DOI:10.1016/j.coldregions.2012.05.014.

Thompson, T., 1981. Proposed Format for Gridded Sea Ice Information (SIGRID). Unpublished report prepared for the World Climate Programme.

Timco, G.W., Burden, R.P., 1997. An analysis of the shapes of sea ice ridges. Cold Reg. Sci. Technol., 25 (1) (1997), pp. 65-77. DOI:10.1016/S0165-232X(96)00017-1.

Tõns, T., Erceg, S., Ehlers, S., Leira, B. J., 2014. Ice condition database for the Arctic Sea. Proceedings of the ASME 2014 33rd International Conference on Ocean, Offshore and Arctic Engineering. OMAE2014-23761.

Tucker, W.B., Ackley S.F., 1998. Analysis of Arctic ice draft profiles obtained by submarines. U.S. Army's Cold Regions Research and Engineering Laboratory (CRREL), Hanover, New Hampshire.

Valkonen, J., Riska, K., 2014. Assessment of the feasibility of the Arctic Sea transportation by using ship ice transit simulation. Proceedings of the ASME 2014 33rd International Conference on Ocean, Offshore and Arctic Engineering. OMAE2014-24188.

Wadhams, P., Horne, R.J., 1980. An analysis of ice profiles obtained by submarine in the Beaufort Sea. Journal of Glaciology. 25, 401-424.

Wadhams, P., 1984. Arctic sea ice morphology and its measurement, in: Dyer, I., Chryssostomidis, C. (Eds.), Arctic Technology and Policy. Hemisphere Publishing Corp., Washington DC, pp. 179-195.

Williams, E., Swithinbank, C., Robin, G.D.Q., 1975. A submarine sonar study of Arctic pack ice. Journal of Glaciology. 15, 349–362.

WMO, 1970. WMO Sea ice Nomenclature, Volume 1: Terminology and Codes. World Meteorological Organization. Report 259, Geneva.

Wright, B., Hnatiuk, J., Kovacs, A., 1978. Sea ice pressure ridges in the Beaufort Sea. Proceedings of IAHR Ice Symposium (1978).